POLITECNICO DI TORINO

Material Engineering For Industry 4.0

Tesi di Laurea

Bio-based polyimine vitrimer

Relatori

Prof. Massimo Messori

Dr. Camilla Noè

Candidato

Mahsa Torabi Yeganeh

Anno Accademico 2024-2025

Abstract

This thesis is focused on the synthesis and the characterization of a polyimine based on vanillin derivative.

As illustrated in Figure 1, vanillin reacted with 4,4'-oxydianiline (ODA) to produce the intermediate monomer, V-ODA (vanilline-4,4'-oxydianiline), which was subsequently used for polymer synthesis. In this reaction the ethanol was used as the solvent and the reaction take 6 hours at 80°C, finally the V-ODA separated by filtration and left to dry for 24 hours.

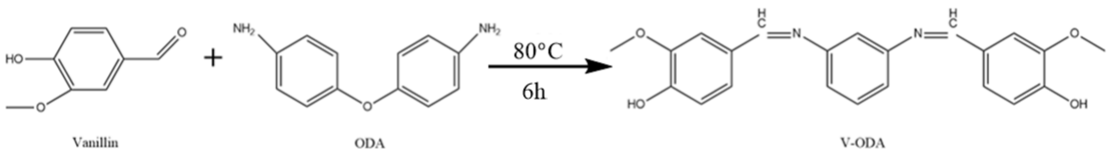

Figure 1 Scheme of V-ODA monomer synthesis

The structure of V-ODA confirmed by ^{1}H NMR and FTIR analyses. Thermogravimetri analysis (TGA) showed good thermal stability, and Differential Scanning Calorimetry (DSC) confirmed the absence of residual solvent.

To synthesize Epoxy V-ODA (Figure 2) the synthesized V-ODA was reacted epichlorohydrin (ECH) at 110 °C and stirred for 30 minutes. To separate the desired epoxy the dichloromethane (DCM) and distilled water were added to form a two-phase system and extract water soluble impurities. Subsequently, to remove residual moisture anhydrous $MgSO_4$ was used. Finally, hexene was introduced to aid to remove of remaining ECH before rotary evaporation.

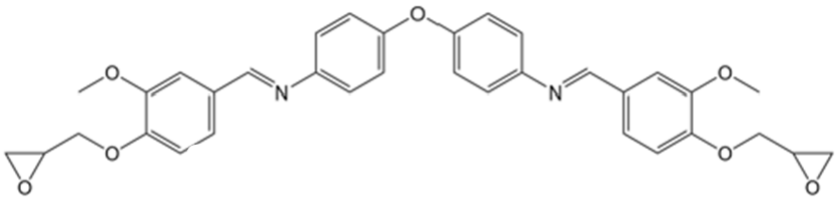

Figure 2 EV-ODA structure

FTIR analysis of EV-ODA confirmed the successful attachment of the epoxy groups, as well as the disappearance of the hydroxyl and amine groups originally present in V-ODA. TGA revealed degradation temperature of 270°C, indicating high thermal stability. DSC analysis showed a broad endothermic peak around 137 °C, which is probably related post-curing of the material.

In crosslinking step, EV-ODA was dissolved in dimethyl sulfoxide (DMSO) and Ytterbium (III) trifluoromethanesulfonate was added as the thermal initiator. Different amount of thermal initiator (3%wt, 4%wt and 5%wt) was added. The mixture was cured at 80 °C for 24 hours.

FTIR analysis, which performed after the curing, confirmed the presence of imine groups and disappearance of epoxy ring in the polymer network; however, no significant differences were observed in the spectra of samples containing different amounts of thermal initiator. Therefore, the further test and analysis of this study was performed by using a 3%wt of the thermal initiator for each sample.

Dynamic mechanical analysis (DMA), was initially performed over a temperature range of -15°C to 330°C. In the first trial, the storage modulus increased unexpectedly around 100°C, which might be due

to post curing. In the second and third trials, the storage modulus decreased as the temperature increased. The glass transition temperature (Tg) increased from 247°C in the second trial to 298°C in the third trial which might be due to increasing crosslinking occurring during the heating cycles.

Stress relaxation test was performed at 150°C on circular sample under 5%strain. The material showed significant stress relaxation after 1h, which indicate network rearrangement through imine bond exchange.

Finally, reprocessability of material evaluate. Solvent free EV-ODA with 3%wt of thermal initiator hot pressed for 15 minutes at 150°C, which resulted in the formation of a very thin and homogenous film. After each tensile test, the broken material hot pressed at 150°C, and in all four cycles, the resulting film was homogeneous. Despite the brittleness of film, it can withstand applying a load for a few moments before failure.

Table of content

List of figures

List of tables

1 Introduction

This thesis has synthesis and characteristic of Vitrimeric Epoxy-Amine Polyimine Networks Schiff Base Derived from Vanillin. This project was developed entirely in the department of DISAT (Politecnico di Torino).

The project is focused on synthesizing vitrimer based on di-amine vanillin with different amounts of curing agents, followed by its characterization.

The second section of thesis describes the synthesis methods. Subsequently, the chapter “Result and Discussion” describes the quality characteristics and mechanical characteristics of obtained product.

Lastly, the conclusions regarding the work done are exposed.

1.1 Polymers

The term "polymer" comes from Greek, meaning "many parts" which describes their fundamental structure composed of repeating monomeric units. These monomers are bonded and form the long molecular chains which define the polymeric materials. Most of the polymers are petroleum-based precursors and are based on carbon chemistry. A key property of polymers is their high molecular weight, which influences on their physical and mechanical properties significantly. While the term "plastics" is often used synonymously with synthetic polymers it is not entirely accurate, as not all synthetic polymers exhibit permanent deformability, which is typically plastic characteristic [1].

The production of polymeric materials has increased substantially over the decades, driven by their widespread use across various industries. Between 1950 and 2023, global plastic production surged to 413.8 million metric tons (Figure 3) [2]. This continuous increase is primarily attributed to the advantageous properties of polymers, including cost efficiency, durability, safety, and ease of processing. Additionally, their lightweight nature, resistance to degradation, adaptability in appearance, and excellent manufacturability have made them a preferred alternative to traditional materials in numerous applications [2], [3].

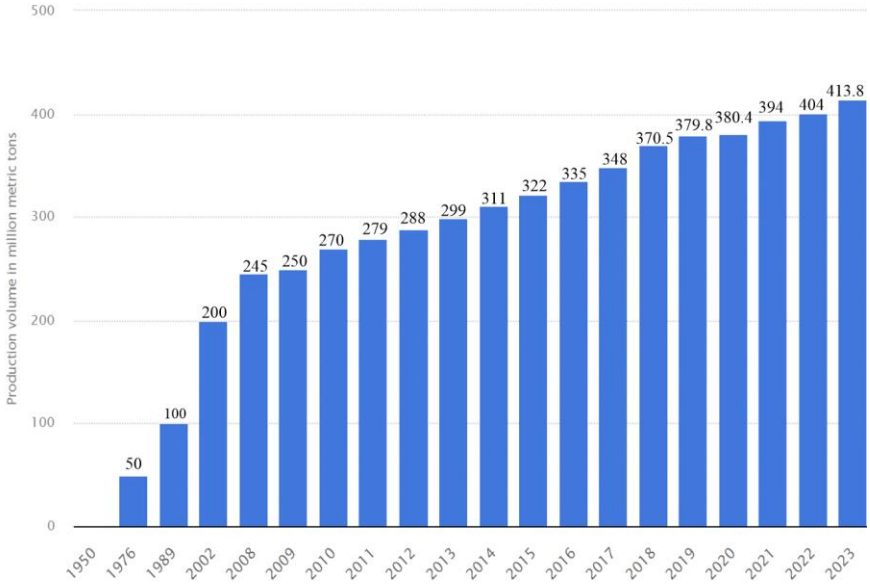

Figure 3 Annual production of plastics worldwide from 1950 to 2023 [4]

While the 20th century was defined by the rapid growth in material production and consumption, the 21st century is increasingly recognized as the era of recycling and focused on sustainability instead of mass production and consumerism. Considering high amount of waste, nearly 40%, having a lifespan of less than a month, the accumulation of waste products has led to substantial environmental issues. As a result, recycling has become very critical, aiming to reduce waste generation and promote sustainability. Waste is mainly managed through incineration or landfill, but recycling is increasingly favoured due to regulations, costs, and environmental concerns. By reprocessing the material in recycling the need for extraction virgin resources decrease significantly which means that recycling conserve the resources. Subsequently, using reprocessed material in manufacturing consumed fewer energy rather than extracting raw material and use it for manufacturing which leads to lower CO_2 emission [5].

1.2 Thermoplastics and thermosets

Properties of polymers are highly dependent on temperature. The mobility of polymer chains changes according to temperature changes. The critical temperature at which polymers transfer from rigid and glassy state to a soft and rubbery state is known as the glass transition temperature (Tg). Glass transition temperature is affected by chemical structure, crosslink density, and molecular weight [6].

Polymers classify based on different criteria such as chain topology, polymerization mechanism, their origin. One of the common polymer classifications is based on their respond to heat, which is directly affected by topology of the polymer. In this category the polymers classify into three groups: thermoplastics, elastomer, and thermosets (Figure 4) [7].

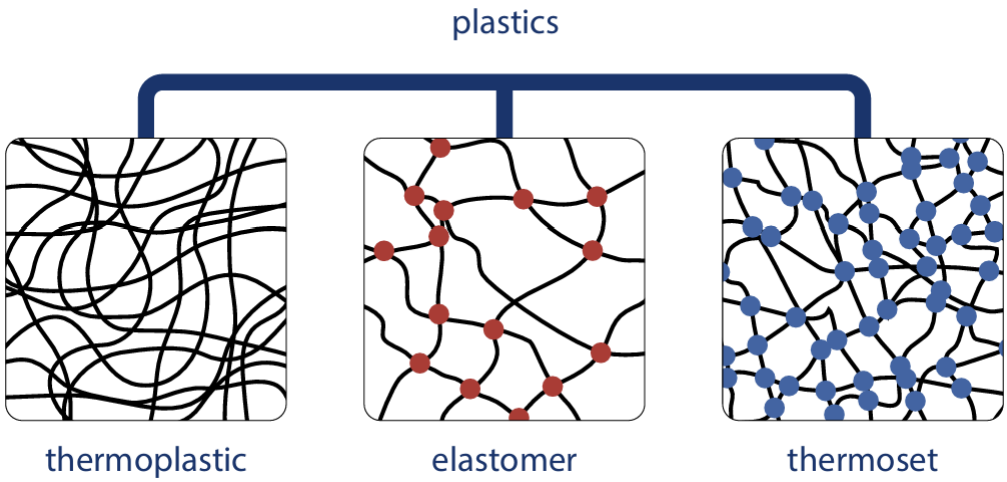

Figure 4 Different groups of polymers [8]

Thermoplastics are group of polymers that can soften and reshape multiple time by reheating and then harden by cooling. In this group of polymers, there is not permanent chemical bonds between the chains, which allows them to behave like viscous liquid under heat and pressure [9].

Elastomer is a type of polymeric material which exhibits both elastic and viscous properties. Elastomers contain long and flexible polymer chains that are loosely held together by weak intermolecular forces, allowing them to stretch and return to their original shape. The weak bonding between the chains gives them their characteristic elasticity and softness. They can be sourced from natural origins, such as natural rubber harvested from rubber trees. Alternatively, they can be produced synthetically using raw materials based on platinum or other chemical compounds. Synthetic elastomers offer more controlled properties and can be tailored for specific industrial needs [10]. Elastomers have the ability to rapidly revert to their original shape and dimensions following by removal of an applied deforming force [11]. They are predominantly utilized in applications such as tires, seals, and as impact modifiers for thermoplastics. These materials demonstrate significant resistance to impact, even at low temperatures [12].

Thermosets are a category of polymers that are synthesized through the combination and subsequent chemical reaction of fluid precursors within a mould. Upon the reaction of these precursors, a crosslinked network is established, resulting in a material that cannot flow upon exposure to heat [12]. The distinct thermal behaviour exhibited by thermosets and thermoplastics can be attributed to their respective chemical structures. Thermoplastics consist of linear polymers that exist in either a semicrystalline or amorphous glass state when solid. Upon heating beyond the melting point of the

crystalline regions (as observed in semicrystalline thermoplastics such as polyethylene) or surpassing the glass transition temperature (as seen in amorphous thermoplastics like atactic polystyrene), the polymer chains gain mobility, resulting in flow. Conversely, thermosets are characterized by their cross-linked polymer structure, which maintains its solid state as long as the covalent bonds remain intact [13]. These thermosetting polymers, which attain a permanent shape during the curing process, play a significant role in contemporary plastics and rubber industries. They account for approximately 20 percent of the total polymeric materials produced globally, with an annual production volume estimated at around 65 million tons [14]. The growing emphasis on environmental sustainability, particularly regarding the conservation of finite resources and the management of waste disposal, has resulted in heightened advocacy for the recycling of materials once they have reached the end of their useful life[15]. Nevertheless, cross-linked polymers, which are predominantly derived from petroleum-based feedstocks characterized by nondegradable hydrocarbon backbones, present significant challenges to long-term sustainability efforts [16].

There are some specific thermosetting polymers which can undergo chemical degradation, that facilitate their removal. Various chemical strategies have been suggested to address this issue, including the integration of disulfide-cleavable bonds within the hardener formulation. These bonds can be effectively degraded by using solvent mixtures which includes acids [17]. An alternative approach involves utilizing epoxy precursors that incorporate ester functional groups, such as cycloaliphatic epoxies, which are synthesized via the esterification of cycloaliphatic acids with α-terpineol, followed by the epoxidation of double bonds. Additionally, the use of anhydrides derived from diacids has been proposed as hardeners to enhance the chemical and thermal reworkability of these materials at moderate temperatures [18], [19].

Another long-term approach to facilitate the recycling and reuse of thermosetting polymers involves substituting traditional chemical cross-linking with reversible covalent bonds or robust non-covalent interactions. Although numerous reversible reactions may be evaluated as potential methods for incorporating reversible covalent bonds into thermosets, the options that exhibit both ease of reversibility and the ability to be repeated are notably limited [20].

1.3 Covalent Adaptable Networks

Adaptable networks are materials characterized by dynamic crosslinks that respond to specific stimuli, facilitating recyclability while preserving numerous advantageous properties associated with thermosetting polymers [21].

Covalent Adaptable Networks (CANs) are defined as networks that contains a sufficient number and topology of reversible covalent bonds, enabling the cross-linked network structure to undergo chemical responses to external stimuli. This respond occurs without permanent damage to the network and preserving the original bond density while allowing material structural rearrangement [20].

CANs can be categorized into two distinct groups based on their exchange mechanisms (Figure 5). The first category employs a dissociative cross-link exchange mechanism; wherein chemical bonds are initially cleaved before being reformed at different locations [22]. When crosslinks are disrupted, the density of crosslinks within the network diminishes, potentially resulting in a loss of network connectivity and, in extreme cases, complete depolymerization. The specific structure of the dissociative crosslinking agent can influence whether the network disruption yields free monomers or unbound polymer chains. In either scenario, the polymers can be reprocessed and reshaped, with the re-establishment of crosslinks facilitating the recovery of the original mechanical properties [23].

An associative dynamic CANs shows constant crosslink density during bond exchange process, as seen in Figure 5, the bond breaking and bond reformation occurs simultaneously. Due to conservation of crosslink density during this bond exchange, the minimum macromolecular structure change happens. In contrast, the dissociative dynamic covalent adoptable networks show more structural change during bond exchange due to crosslink density change [24].

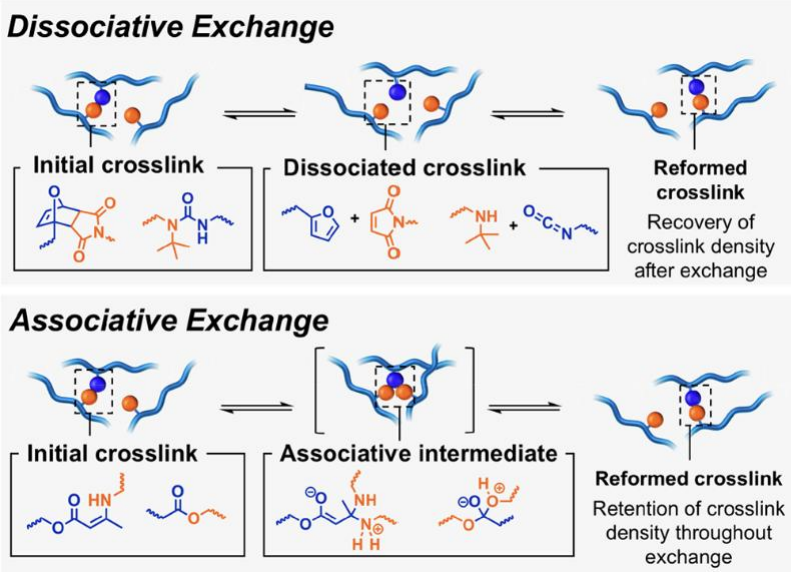

Figure 5 CANs are categorized into two distinct groups: dissociative and associative exchange

Associative process is a characteristic of the recently developed "vitrimer" materials, which demonstrate suitable properties for high-performance applications [25].

1.4 Vitrimers

In 2011, Leibler and co-workers introduced a class of polymeric materials termed vitrimers**,** based on associative CANs[26]. Unlike dissociative CANs, vitrimers feature a permanent chemical network with dynamic covalent bonds that enable the material to undergo topological rearrangement while maintaining a constant number of crosslinks at all temperatures below degradation [7], [23]. This behaviour arises from thermally activated exchange reactions, where dynamic covalent units undergo degenerate processes—meaning the forward and reverse reactions are equilibrium-governed with a thermodynamic constant of 1. As a result, vitrimers retain their bond count regardless of temperature, distinguishing them from other dynamic networks that lose connectivity upon heating [7].

When heated, vitrimers transition from a viscoelastic solid to a viscoelastic liquid**,** allowing them to flow and be reshaped without losing structural integrity [23]. This unique property comes from the temperature-dependent exchange of dynamic covalent bonds, which allows network rearrangement while preserving crosslink density.

Unlike traditional polymer networks, vitrimers retain their dynamic covalent network integrity over a wide range of temperatures (up to degradation temperature), which facilitates distinctive interactions with solvents. Despite they may swell in chemically inert solvents, they do not dissolve in them, even at elevated temperatures. Unlike conventional thermosets with fixed crosslinks, vitrimers exhibit higher swelling ratios due to their ability to undergo bond exchange [22].

Vitrimers demonstrate a distinctive viscoelastic behaviour that is defined by two interrelated transition temperatures: the glass transition temperature (Tg) and the topology-freezing transition temperature (Tv). The glass transition represents the initiation of long-range segmental motion as the material transfer from a rigid glassy state to a rubbery state, similar to the traditional polymers. However, vitrimers demonstrate an additional transition at Tv, where the timescale of dynamic bond exchange reactions becomes shorter than the timescale of material deformation. Below T_v, the material behaves as a viscoelastic solid with effectively frozen topology, whereas above T_v, the accelerated bond exchange facilitates the stress relaxation and macroscopic flow, leading to viscoelastic liquid behaviour. Conventionally, T_v is defined as the temperature at which the viscosity reaches 10^{12} Pa.s, indicating the practical threshold for network reconfiguration. This dual-transition behaviour fundamentally makes vitrimers distinguishable from conventional polymers, as it allows them to combine the dimensional stability and solvent resistance of thermosets below T_v with the reprocessability and stress-relaxation capabilities of thermoplastics at temperature above T_v [22].

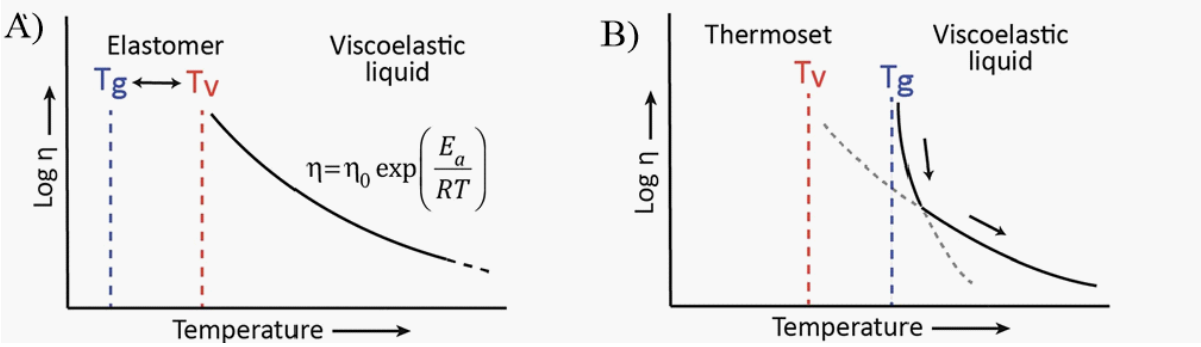

Figure 6 Viscoelastic behaviour of vitrimer with A) Tg<Tv, follows the Arrhenius law, B) Tv<Tg

In systems where Tg < Tv (as illustrated in Figure 6.A), initial applying heat results in transition from glassy region to rubbery state at Tg, where the material behaves like a conventional elastomer with effectively frozen network topology due to slow bond exchange. Further heating above Tv accelerates exchange reactions, leading material to transfer into a viscoelastic liquid which flow follows the Arrhenius-type viscosity behaviour. Conversely, when Tg > Tv (Figure 6.B), the network dynamics are primarily constrained by segmental mobility rather than kinetic of exchange. Below Tg, both segmental motions and bond exchanges are suppressed, and resulting in freezing network structure. Above Tg, the initial rearrangements of the network are limited by the mobility of polymer segments, exhibiting WLF-type viscosity behaviour, which describes the rapid drop in viscosity near Tg due to increasing chain mobility, until higher temperatures where exchange reactions become dominant and Arrhenius kinetics become prevalent. In these cases, Tv represents a hypothetical transition point, while the practical network freezing is determined by Tg, which imposes limitation on segmental mobility [22].

2 Experimental

2.1 Material

Vanillin, 4,4’-Oxydianiline (ODA), Ethanol, Epichlorohydrin, Benzyl trimethylammonium chloride($C_{10}H_{10}ClN$), Dichloromethane, Distilled water, Anhydrous MgSO4, Hexane, Dimethyl sulfoxide, Ytterbium (III) trifluoromethanesulfonate($(CF_3SO_3)_3Yb$).

2.2 Synthesis

2.2.1 Monomer synthesis

The synthesis of the monomer was achieved according to the literature procedure [27]. The monomer V-ODA was synthesized by reacting vanillin with 4,4ˋ-Oxydianiline (ODA) in ethanol as a solvent. The reaction stoichiometry was based on the functional groups of the reactants, amine groups in ODA and aldehyde groups in vanillin (For each mole of diamine (ODA), 2 moles of vanillin were used for balanced reactivity).
The quantities of vanillin and ODA were based on a molar ration 2:1.
The synthesis of V-ODA was conducted using a three-neck reaction flask. To provide uniform heat distribution, a Pyrex crucible was filled with sand and used as a thermal medium to surround the reaction flask. The crucible was then placed on a heater equipped with a magnetic stirrer, enhancing the even transfer of heat throughout the reaction.

The three-neck flask was placed centrally in the crucible and secured with a stand and clamps, and the lateral necks of the flask were sealed with appropriate plastic caps to prevent any external contamination or lose of reactant. Ethanol was then added to the flask as the solvent, and a magnetic stirrer was placed inside to facilitate continuous mixing during the reaction.

Following this, the required amounts of 4,4'-Oxydianiline (ODA) and vanillin were accurately weighed according to stoichiometric calculations and added to the flask. A vertical condenser was attached to the central neck of the flask to prevent the evaporation of the solvent during heating. The condenser was connected to a water supply with a plastic tube attached to the lower inlet, allowing water to flow in from the bottom and exit from the top outlet.

To monitor the temperature, a thermometer was inserted into the sand within the crucible, positioned close to the reaction flask, as the reaction was maintained at 80 °C (Figure 7).

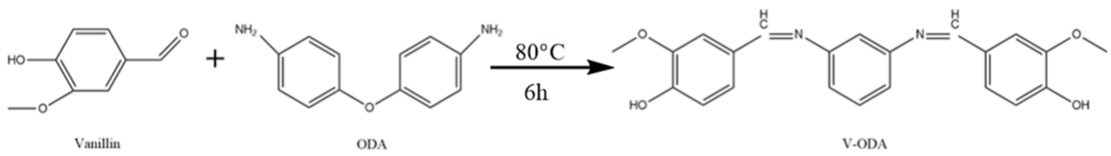

Figure 7 Synthesis reaction of V-ODA

The reaction was allowed to continue for six hours. After this period, the heater was turned off, and the setup was left to cool to room temperature. Once cooled, all instruments were detached, and the filtration of V-ODA began. Filter paper was placed inside a funnel positioned over a Buchner flask to separate V-ODA from the solvent. A plastic Pasteur pipette was used to carefully remove the reaction mixture from the flask and pour it onto the filter paper, this allowed the solvent to pass through, leaving the solid V-ODA on the filter paper (Figure 8).

Figure 8 Filtering synthesized V-ODA

Following filtration, the solid V-ODA was washed three times with ethanol to remove any unreacted materials. The washed V-ODA and the solvent was left to evalopare under the fumehood. Finally, the dried V-ODA was placed into plastic tubes, weighed, and the yield was calculated (Table 1).

Table 1 Summary of used material in the monomer synthesis reaction

Sample	Vanillin (g)	ODA (g)	Ethanol (mL)	V-ODA (g)	Process yield (%)
V-ODA1	7.6	5	100	3.5	30
V-ODA2	7.6	5	100	8.794	80.3
V-ODA3	7.6	5	100	7.997	73
V-ODA4	12	7.896	100	14.966	81

Figure 9 shows the appearance of the sample after filtration and drying.

Figure 9 Synthesized V-ODA samples

2.2.2 Monomer epoxidation

The synthesis of Epoxy-V-ODA was achieved according to the literature procedure [28]. In the second phase, V-ODA was used as a starting monomer to synthesize the epoxy V-ODA. For this process, a 250 mL three-neck round bottom flask was employed, equipped with a magnetic stirrer and a thermometer to monitor the reaction temperature. To ensure uniform heat distribution throughout the mixture, as in the first phase, a sand bath with a crucible was utilized. The flask was charged with 8.5 g (18.1 mmol) of V-ODA and 100.7 g (1.1 mol) of epichlorohydrin (ECH). The heater was then turned on, and the magnetic stirrer began to stir the mixture until the temperature reached 110°C. Once the temperature was achieved, a small amount of benzyl trimethylammonium chloride (BTMA, 0.34 g) was added as a phase transfer catalyst to enhance the reactivity and improve the reaction yield. The reaction continued for 30 minutes, and after this period, the mixture was allowed to cool down to room temperature (Figure 10).

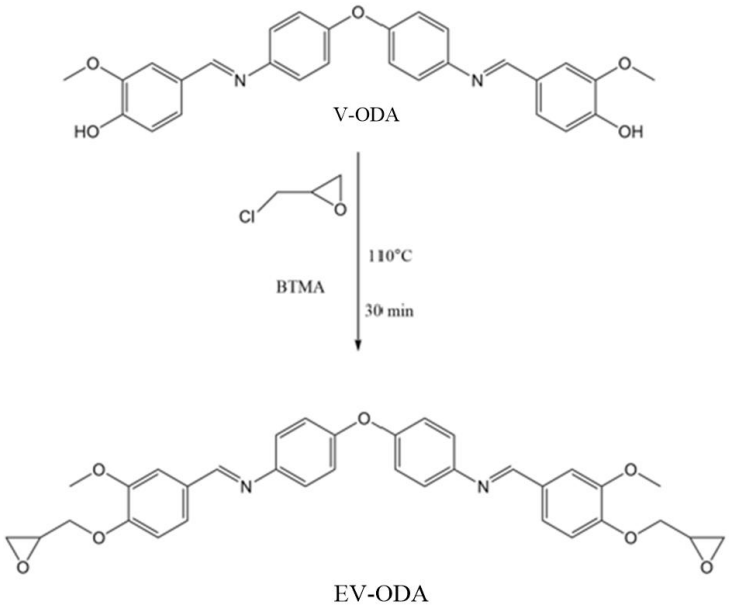

Figure 10 Synthesis of Epoxy V-ODA

At this step, the reaction mixture contained unreacted epichlorohydrin (ECH), the desired epoxy V-ODA, catalyst residues, and potential byproducts. To separate the desired product, an extraction process was carried out. Initially, 50 mL of dichloromethane (DCM) was added to the mixture, resulting in a two-phase system. The organic phase, which included DCM, EV-ODA, and ECH, separated from the aqueous phase, which contained catalyst, water-soluble impurities, and byproducts. To further remove the impurity, distilled water was added to the mixture, facilitating the extraction of water-soluble contaminants. Due to their different densities and immiscibility, the two phases formed distinct layers, with the aqueous phase on top and the organic phase at the bottom. The organic layer was then carefully separated.

After the separation of the organic phase, anhydrous MgSO4 was introduced as a strong moisture absorbent to eliminate any residual amounts of water that might remain in the organic phase. The hydrated MgSO4 was subsequently separated through filtration, leaving the organic phase completely free of moisture.

Next, the solvents (ECH and DCM) needed to be removed. A rotary evaporator was used for this purpose (Figure 11). Hexene was also added to help remove any remaining ECH, as it reduces the solubility of

ECH in the organic phase. In the rotary evaporator, solvents evaporate based on their boiling points. The vacuum was applied to the system, causing the DCM to evaporate first due to its lower boiling point compared to ECH. As the temperature was gradually increased, ECH also started to evaporate. Both DCM and ECH were removed gradually as the pressure was lowered. The vapours then entered the condenser, where they cooled and condensed back into liquid form, collecting in a separate receiving flask. Ultimately, only the solid EV-ODA product remained in the original flask.

Figure 11 Rotary evaporator; A) Solvent collector flask after its evaporation, B) Original flask

The prepared epoxy is shown below:

Figure 12 Epoxy V-ODA

2.2.3 Polymer crosslinking

The crosslinking reaction of the EV-ODA_involved the ring-opening of the EV-ODA using dimethyl sulfoxide (DMSO) as a solvent and a thermal initiator [28]. The maximum solubility of EV-ODA in DMSO was 250 mg/Ml.

Measured amounts of EV-ODA and DMSO were placed into glass vials, each containing a magnetic stir bar. The vials were positioned in a Pyrex crucible which were filled with sand to ensure uniform heat distribution. The crucible was placed on a heater equipped with a magnetic stirrer, and the temperature was carefully maintained at 70°C to prevent undesired changes to the chemical bonds (Figure 13). The mixture was stirred continuously until a homogeneous solution was obtained.

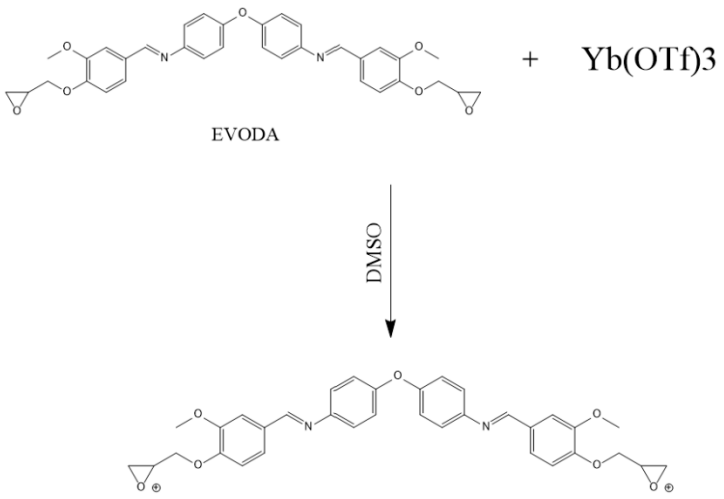

Figure 13 Cationic monomer

Once the EV-ODA was completely dissolved in DMSO, varying amounts of the thermal initiator, Ytterbium (III) trifluoromethanesulfonate (Figure 14), were added to each vial (Table 2). The mixtures were stirred for a few additional minutes to ensure the complete dissolution of the thermal-initiator.

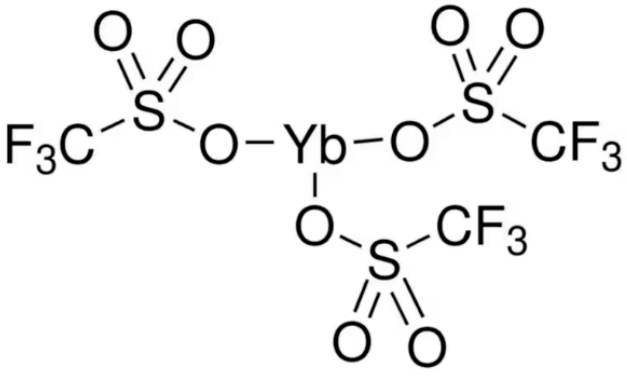

Figure 14 Thermal initiator structure

Table 2 Compositions of polymer samples

	Sample 1	Sample 2	Sample 3	Sample 4
EV-ODA(g)	0.25	0.25	0.25	0.25
DMSO(g)	1.2	1.2	1.2	1.2
Thermal initiator(%wt)	3	4	5	0

The resulting solutions were then poured into rectangular moulds (Figure 15) and placed in an oven maintained at 70°C for 24 hours allowing the crosslinking reaction and the evaporation of the solvent. This process yielded a solid polymeric material, that was subsequently tested.

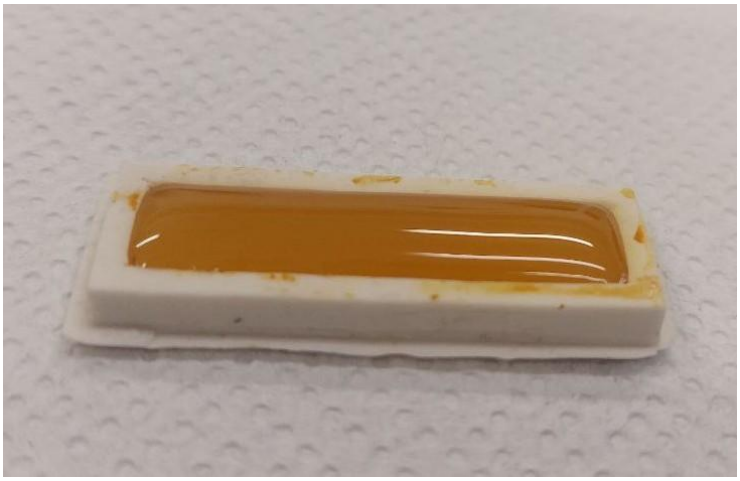

Figure 15 Vitrimer before curing

2.3 Charactrisation methods

2.3.1 Chemical analysis

2.3.1.1 1H-NMR

Nuclear Magnetic Resonance (NMR) spectroscopy is a powerful technique for elucidating molecular structures by exciting transitions between nuclear spin states and detecting the resulting energy absorption and emission. The energy levels observed in NMR arise from the interaction of nuclear spins with surrounding magnetic fields, which are influenced by the chemical environment and the distribution of electrons around the nucleus.

The separation of these energy levels, which is observed as the "chemical shift", depends on the local chemical environment, while the number of energy levels is affected by interactions between nuclear spins, known as spin-spin coupling. When a nucleus is subjected to a magnetic field, its magnetic moments align in quantized orientations, leading to formation of discrete energy levels, a phenomenon known as Zeeman splitting.

In NMR, all transitions between energy levels are not allowed. As a result, even nuclei with multiple energy levels, such as quadrupolar nuclei, typically exhibit a single resonance due to the equal spacing of these energy levels.

At the Larmor frequency, nuclear spins can absorb energy to transition from lower to higher states or emit energy when they return to lower energy states. The intensity of the resulting NMR signal is directly correlated to the difference between the number of these energy levels, which is affected by the gyromagnetic ratio (γ). Nuclei with lower γ values produce weaker signals, which is one of the limitations in NMR sensitivity.

The NMR signals are influenced by two different types of electron-induced fields: the first one generated by electron circulation, which opposes the applied magnetic field, and another produced by electrons in excited states, which can either provide shielding or deshielding effects on the nucleus. This interaction between electrons and nucleus, known as the paramagnetic term, contributes to variations in shielding, thereby affecting the observed resonance frequency.

To standardize measurements across different spectrometers, chemical shifts are reported as a fractional frequency shift from a reference compound, measured in parts per million (ppm). This chemical shift value, denoted as δ, increases as shielding decreases and is calculated using the equation:

$$\delta=(\nu_{ref}-\nu_{observed}/\nu_{ref})\times 10^6$$

where $\nu_{observed}$ is the observed resonance frequency, and ν_{ref} is the reference frequency [29].

2.3.1.2 FTIR

Fourier Transform Infrared (FTIR) spectroscopy is a powerful analytical technique for identifying chemical bonds within a molecule by producing an infrared absorption spectrum unique to each substance, serving as a molecular fingerprint. This method is effective for characterizing both organic and inorganic compounds and can be applied to analyse solids, liquids, and gases. As a vibrational spectroscopic technique, FTIR relies on the interaction between infrared electromagnetic radiation and the sample, offering significant advantages such as high sensitivity, rapid data acquisition, and non-destructive analysis. Compared to dispersive instruments, FTIR spectrometers deliver enhanced energy

throughput, greater sensitivity, and accelerated spectral acquisition, making them particularly suitable for advanced material analysis [30].

The analysis was performed with Nicolet™ iS50 FTIR Spectrometer equipped with an Attenuated Total Reflection (ATR) setup (Figure 16). The sample was positioned on the instrument's crucible and then covered with a pressure anvil, which was secured using a screwdriver. The analysis was conducted within the range of 400–4000 cm^{-1}.

Figure 16 FTIR instrument

2.3.2 Thermal analysis

2.3.2.1 DSC

Differential Scanning Calorimetry (DSC) is widely utilized to investigate the physical characteristics of polymers. This technique facilitates the analysis of thermal events such as melting, crystallization, and mesomorphic transitions, along with the associated changes in enthalpy and entropy. It is also effective for identifying glass transitions and other thermal effects that involve shifts in heat capacity or latent heat [31].

The DSC setup consists of two pans positioned on heaters, with one pan holding the sample to be analysed and the other serving as an empty reference. The temperature is precisely controlled, and the heat supplied to each pan is carefully measured. Typically, less heat is required for the reference pan because it contains no material undergoing thermal transitions, unlike the sample pan, which may absorb or release heat during such processes. The additional heat provided to the sample ensures that its temperature matches the temperature increase of the reference [31].

During the analysis, a graph is generated with the temperature plotted on the x-axis and the heat flow difference required to maintain the same temperature increase on the y-axis, offering insights into the thermal properties of the sample.

DSC test was performed using a DSC 214 Polyma instrument. The sample was studied with heating rate of 10°C/min under nitrogen flow with a purge rate of 50mL/min. The DSC was performed over a temperature range of 25°C to 250°C.

2.3.2.2 TGA

Thermogravimetric analysis (TGA) is a technique used to measure changes in the weight of a sample as a function of temperature or time under controlled conditions. This analysis is performed using a thermogravimetric analyser, which records the weight changes and generates a TGA curve, typically plotting mass against temperature or time. Weight variations in the sample can result from processes such as the evaporation of volatiles, drying, desorption or adsorption, decomposition, or oxidation, depending on the experimental environment [32].

For the TGA test, less than 10 mg of the sample was placed in an aluminium crucible and inserted into the analyser from the top. The analyser is equipped with a precise microbalance to measure the sample's weight changes within a closed furnace. A thermocouple positioned near the crucible ensured accurate monitoring of the sample's temperature. To isolate the sample from the heating elements and cooling coils, a protective tube was used [33]. Argon gas, an inert atmosphere, was supplied at a flow rate of 50 mL/min to prevent oxidation during the test. The temperature was programmed to increase from 25°C to 800°C at a rate of 10°C/min, with the total test duration exceeding one hour.

The analyses were conducted using a Mettler Toledo TGA/SDTA851e instrument (Figure 17) at a controlled heating rate of 10°C/min under an argon atmosphere. To ensure consistency, a purge rate of 50 mL/min was maintained throughout the process, covering a temperature range from 25°C to 800°C.

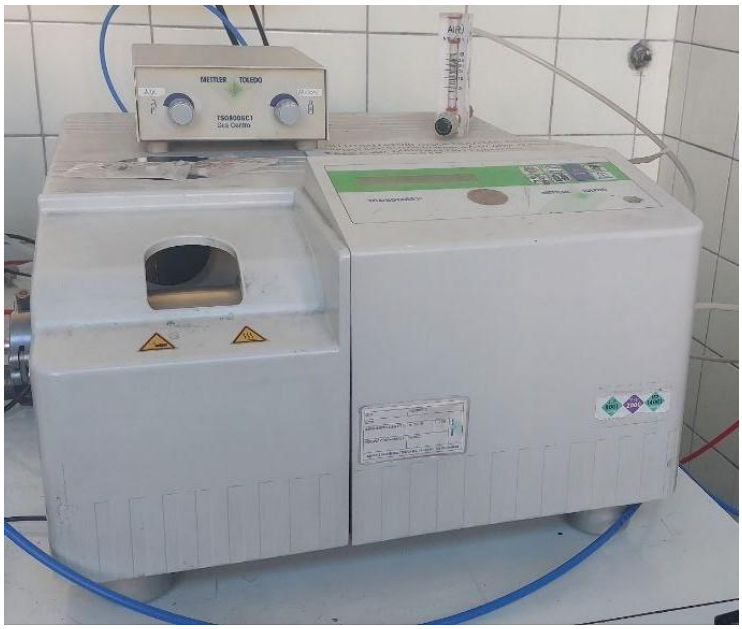

Figure 17 TGA instrument

2.3.3 Mechanical analysis

2.3.3.1 Dynamic mechanical analysis (DMA)

Dynamic mechanical analysis (DMA) performed using the MCR702e Rheometer (Figure 18), has emerged as one of the most powerful tools available for the study of the behaviour of plastic materials [34]. Simply stated, DMA measures the viscoelastic properties of materials by evaluating their behaviour under cyclic stress while varying temperature.

Figure 18 Dynamic mechanical analysis instrument

The DMA results usually include three key parameters:

- Storage modulus (G′): representing the elastic response of the material,
- Loss modulus (G″): reflecting the viscous dissipation of energy, and
- tan δ (G″/G′): the damping factor [35], which tan δ gives information about the energy dissipation of the material under cyclic load. This quantity varies with the state of material, its temperature and the applied frequency.

Since the material lose their modulus at glass transition temperature it is possible to find Tg from DMA. The Tg is detected at the maximum point of tan δ curve [36].

2.3.3.2 Stress relaxation

Stress relaxation refers to the time-dependent reduction in stress experienced by a material when subjected to a constant strain. This behaviour of polymer is studied by applying a fixed deformation to a sample and monitoring the stress (or force) decrease to maintain that deformation over time [37].

Stress relaxation experiment was performed by using dynamic mechanical analysis MCR 702e (Figure 19) in compression mode with circular disc-shape sample.

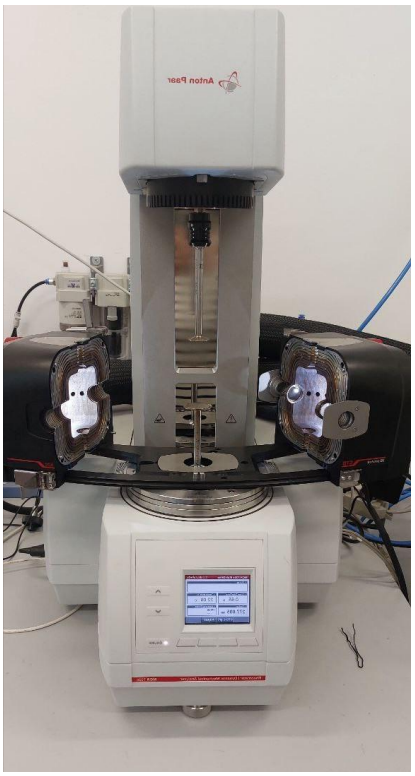

Figure 19 Dynamic mechanical analysis instrument

2.3.3.3 Tensile test

The tensile testing is a destructive mechanical testing technique employed to evaluate essential material properties, including Young modulus, tensile strength and yield strength [38].

This method examines a material's capacity to endure applied stress (force per unit area) by subjecting it to tensile forces until failure occurs.

The behaviour of a tensile specimen in response to the application of increasing stress can be characterized by its elastic and plastic responses. Initially, the specimen experiences elastic elongation as it is subjected to tensile forces. With the continued application of stress, the specimen transitions into a state of permanent deformation, referred to as plastic strain. The stress-strain curve serves as a critical tool for identifying the threshold at which the reversible elastic strain is surpassed, leading to the onset of permanent or plastic deformation. The yield strength is defined as the level of stress required to induce substantial plastic deformation in the material [39].

Samples for tensile test prepared by using Gibitre laboratory press (Figure 20).

Figure 20 Gibitre laboratory press

The tensile test was performed by Instron 5966 universal testing machine (Figure 21), and the tensile force, F_T, recorded. The tensile test was performed by 1mm/min loading velocity and force of 250N.

Figure 21 Universal tensile machine

3 Result and discussion

3.1 Monomer

3.1.1 1H-NMR

The [1]H-NMR spectroscopy was employed to characterize the structure and purity of V-ODA, monomer as illustrated in Figure 22.

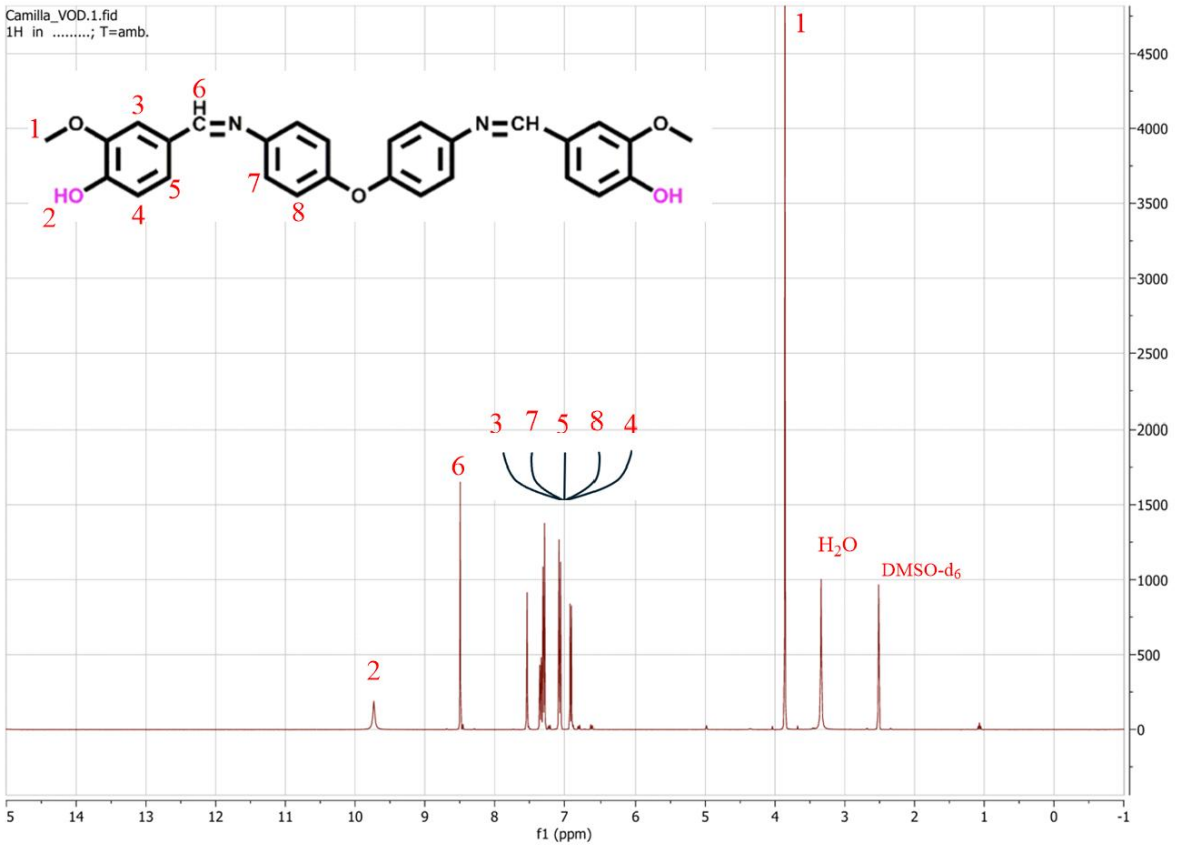

Figure 22 [1]HNMR signals of V-ODA

As it is shown in Figure 22, the peak observed at 9.75 ppm corresponds to the hydroxyl group (H_2), which exhibits a higher chemical shift due to its polar nature. The peak at 8.49 ppm is attributed to the proton of imine group (H_6), indicating the successful formation of this bond. Additionally, the peak at 3.85 ppm is associated with the methoxy group in V-ODA. The peaks within the range of 6.5 to 8 ppm are assigned to the protons of the benzene ring present in the V-ODA structure. Furthermore, the peak near 3.3 ppm suggests the presence of some moisture in the sample or in the solvent. The [1]HNMR results are summarized in Table 3:

Table 3 1HNMR result of V-ODA

Hydrogen number	**Corresponding group**
1	methyl group
2	hydroxyl group
3, 4, 5, 7, 8	benzene ring
6	imine group

3.1.2 FTIR

To further assess the successful synthesis of V-ODA, Fourier Transform Infrared (FTIR) spectroscopy was performed. Triplicates spectra were recorded which exhibited nearly identical peaks across all measurements, thereby confirming the uniformity of the material's structure.

As illustrated in Figure 23, the FTIR spectrum for the first synthesized V-ODA sample shows notable changes, indicating successful bond formation. The peak observed at 3154.75 cm^{-1} in vanillin corresponds to the OH stretching vibration, while the peak at 1661.42 cm^{-1} is associated with the aldehyde (C=O) stretching vibration. Additionally, peaks at 3442.19 cm^{-1} and 1280 cm^{-1} in the spectrum of ODA are attributed to the NH and C–N stretching vibrations of the amine group, respectively. In the V-ODA spectrum, the disappearance of peaks corresponding to the aldehyde and amine groups confirms their complete involvement in the reaction. The emergence of a new peak at 1621.43 cm^{-1}, characteristic of the imine (C=N) group, further supports the formation of the desired Schiff base. Furthermore, the -OH stretching vibration peak shifts from 3154.75cm^{-1} in vanillin to 3504.43cm^{-1} in V-ODAC [27], [40].

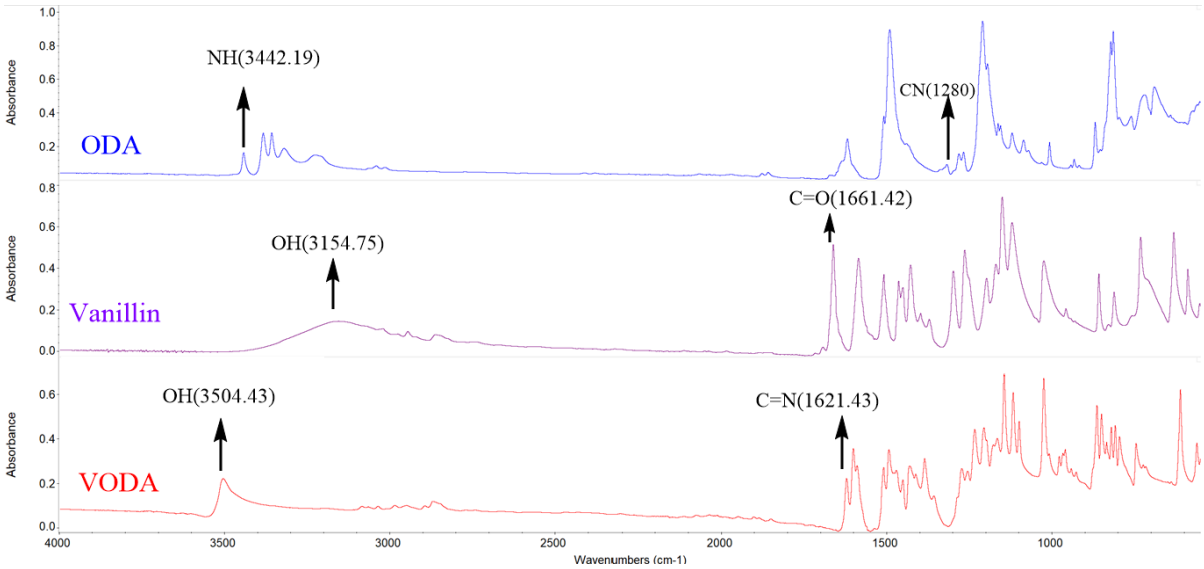

Figure 23 FTIR spectrum for Vanillin, ODA, V-ODA

3.1.3 DSC

DSC analysis was carried out for V-ODA, and the result is shown in Figure 24:

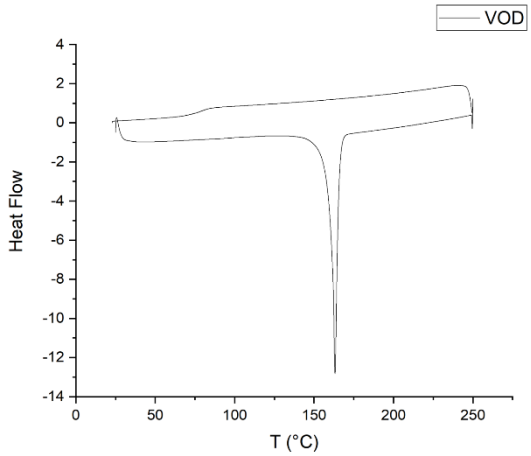

Figure 24 DSC result of monomer

Differential scanning calorimetry (DSC) analysis of the V-ODA monomer revealed a sharp endothermic peak at 163.17°C, indicative of a melting point, and it did not show the endothermic peak related to residual solvent evaporation.

3.2 Epoxy V-ODA

3.2.1 FTIR

Following epoxidation of the monomer, FTIR analysis confirmed both the formation of epoxy rings and imine group and the disappearance of terminal hydroxyl groups (Figure 25).

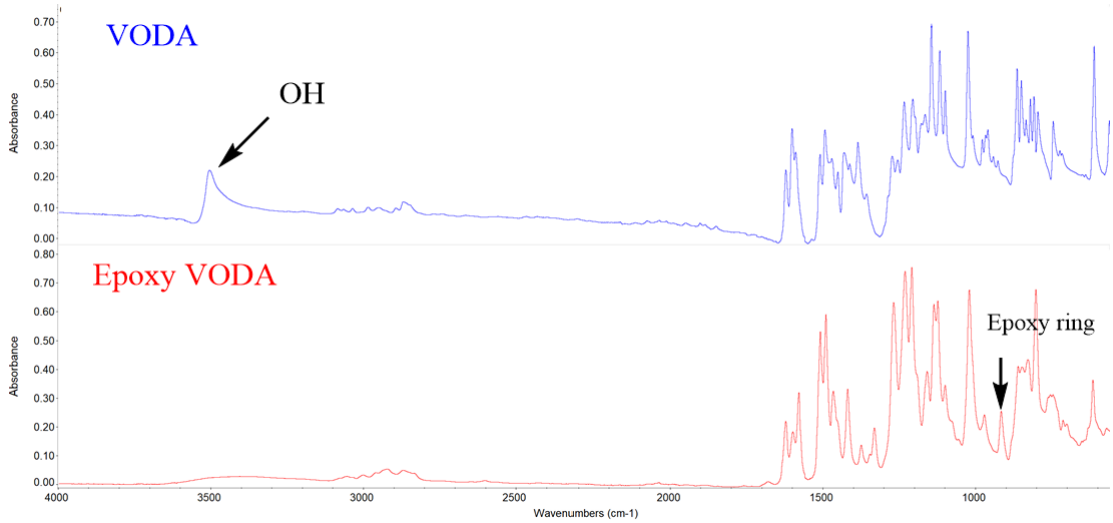

Figure 25 FTIR of EV-ODA and V-ODA

3.2.2 TGA

Thermogravimetric analysis (TGA) was performed on the EV-ODA monomer and on the crosslinked polymer to assess their thermal stability within the designated curing temperature range and to confirm the absence of any decomposition. A sample mass of 8.13 mg of EV-ODA was used for this analysis. The result is shown in Figure 26:

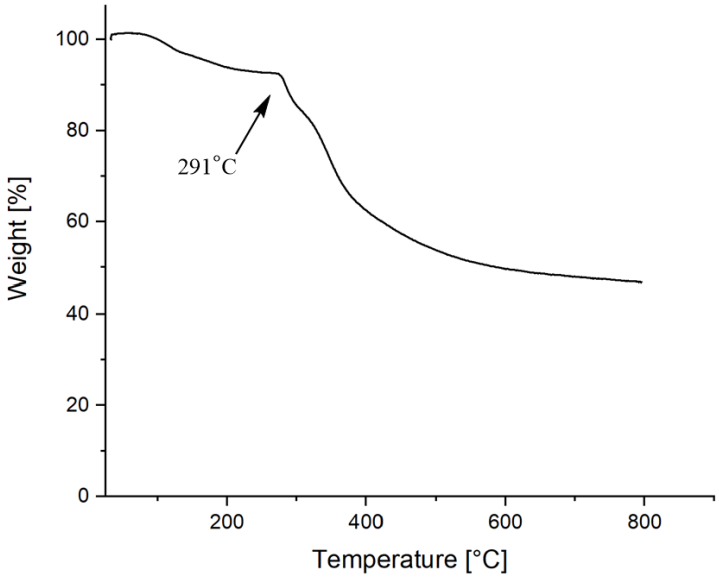

Figure 26 TGA result of EV-ODA

The TGA curve for EVOD indicates a minor decomposition around 100°C, likely due to the removal of residual solvent or moisture. Significant decomposition begins at 291°C, with approximately half of the material decomposing by 800°C. The relatively high residual mass at the end of the test can be due to the formation of a thermally stable char. Based on test result, the EV-ODA are suitable for vitrimer synthesis, as its decomposition temperatures is well above the curing temperature.

3.2.3 DSC

DSC result for EV-ODA is shown in Figure 27:

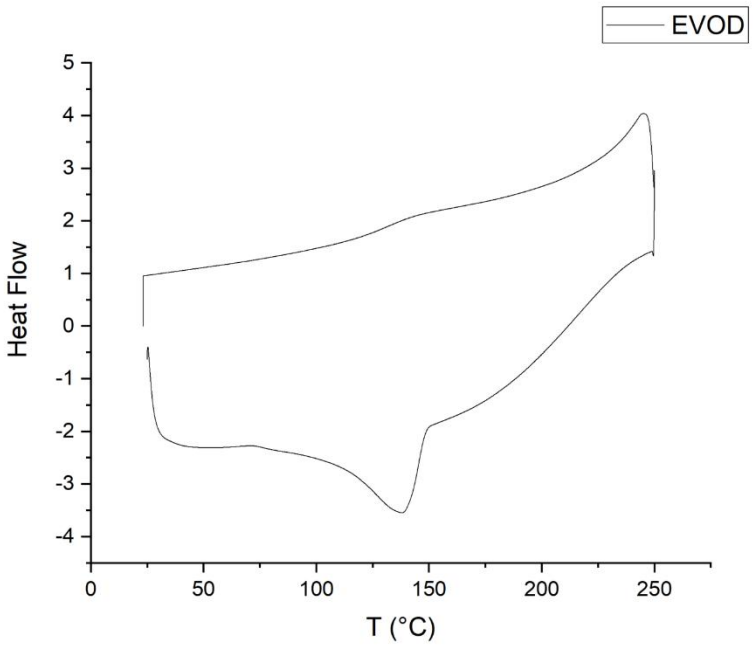

Figure 27 EV-ODA DSC result

The DSC thermogram of EV-ODA exhibited a broad endothermic event centred at 137.89°C, which may be attributed to the evaporation of residual solvents or absorbed moisture. The breadth of this peak suggests a gradual energy absorption process, consistent with the release of volatile components rather than a distinct phase transition.

3.3 Polymer

3.3.1 FTIR

The epoxidized monomer was then thermally cured and polymerized using a thermal initiator. FTIR characterization was subsequently performed to verify the completion of the crosslinking reaction and the final network structure. The result is shown in Figure 28:

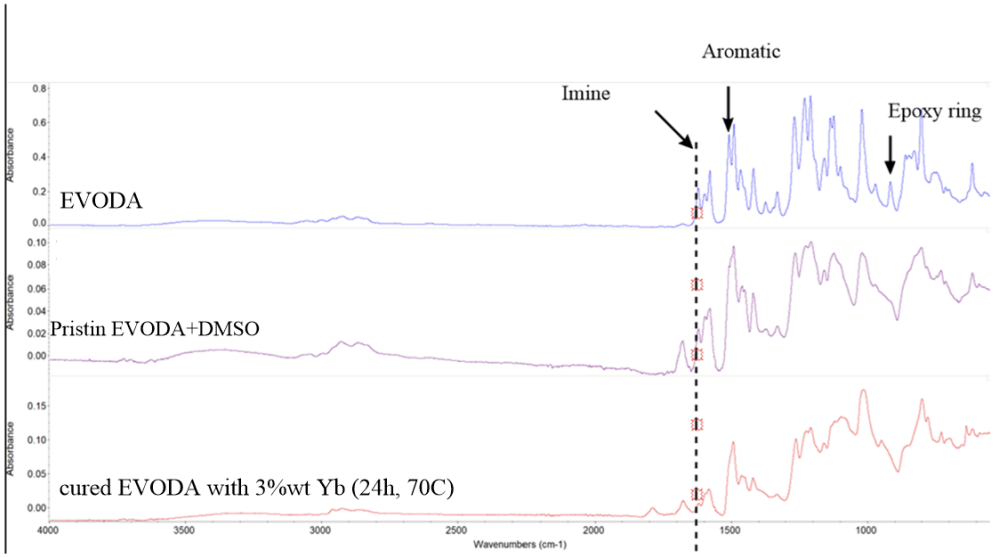

Figure 28 FTIR spectrum of EVOD, EVOD+DMSO, cured EVOD with 3%wt Yb

Based on the FTIR results presented in the Figure 28, cured EV-ODA with 3%wt thermal initiator, resulted the disappearance of the sharp peak at approximately 915 cm^{-1}, associated with the epoxy ring. These observations confirm the successful occurrence of the ring-opening reaction. Additionally, the imine group remained unchanged throughout the process, indicating the retention of these dynamic functional groups in the final material [28].

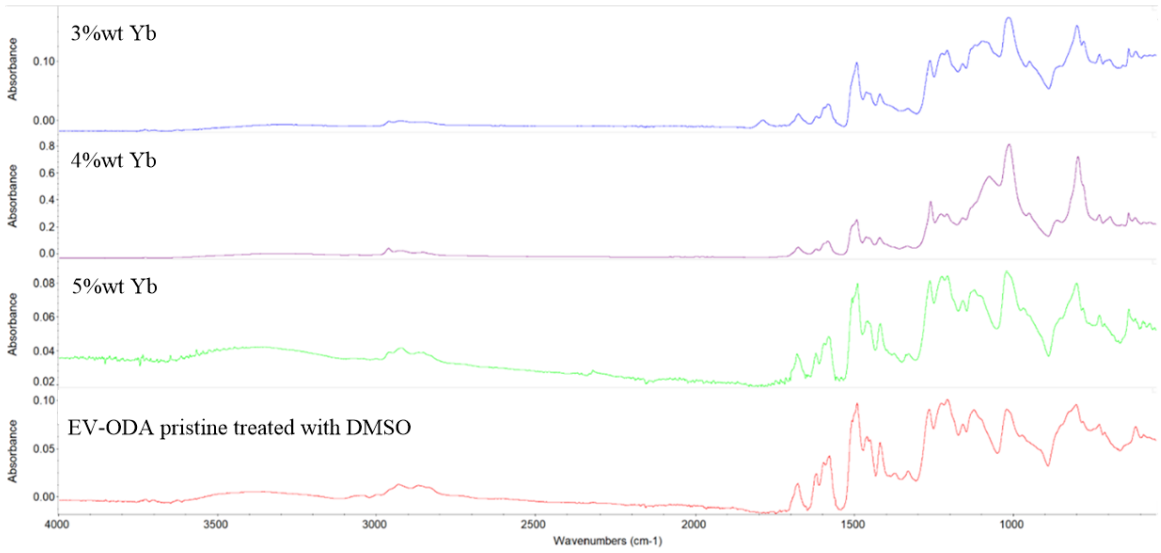

Figure 29 FTIR spectrum of cured EVAD with different amount of thermal initiator

The effect of varying the concentration of photo-initiator on the chemical structure of the samples was investigated using FTIR spectroscopy (Figure 29). All samples displayed characteristic peaks associated with imine groups, confirming their presence across the different formulations. These results suggest that the amount of thermal initiator within the range tested (3–5%) does not have a pronounced effect on the polymerization process, as reflected by the FTIR spectra.

3.3.2 DMA

DMA measurements were conducted in triplicate, from -15°C to 330°C. In the first trial, the temperature range was set from room temperature to 220°C (Figure 30). Initially, the storage modulus decreases with increasing temperature, as expected due to the material softening. However, after approximately 100°C, the modulus began to increase, which might be related to a change of network density and free space [41].

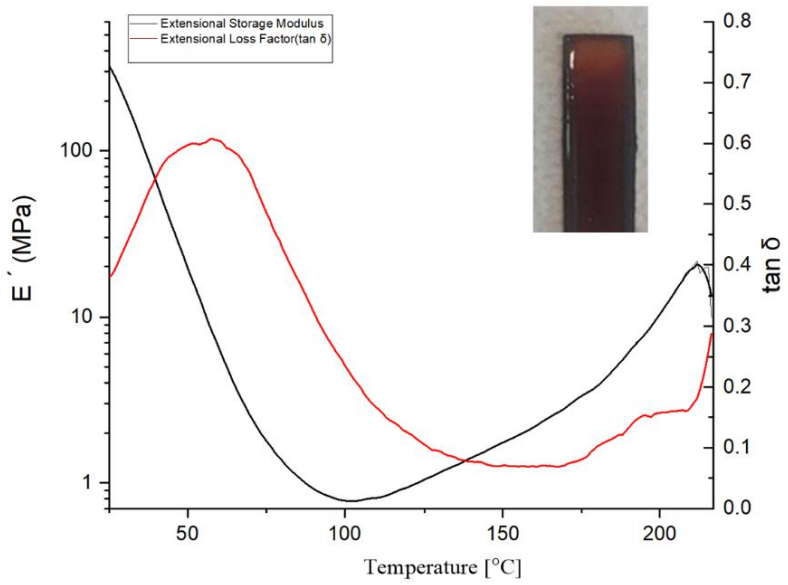

Figure 30 first DMA trial on vitrimer

In subsequent tests, the temperature range was extended from below 0°C (-10°C and -15°C) to 330°C (Figure 31).

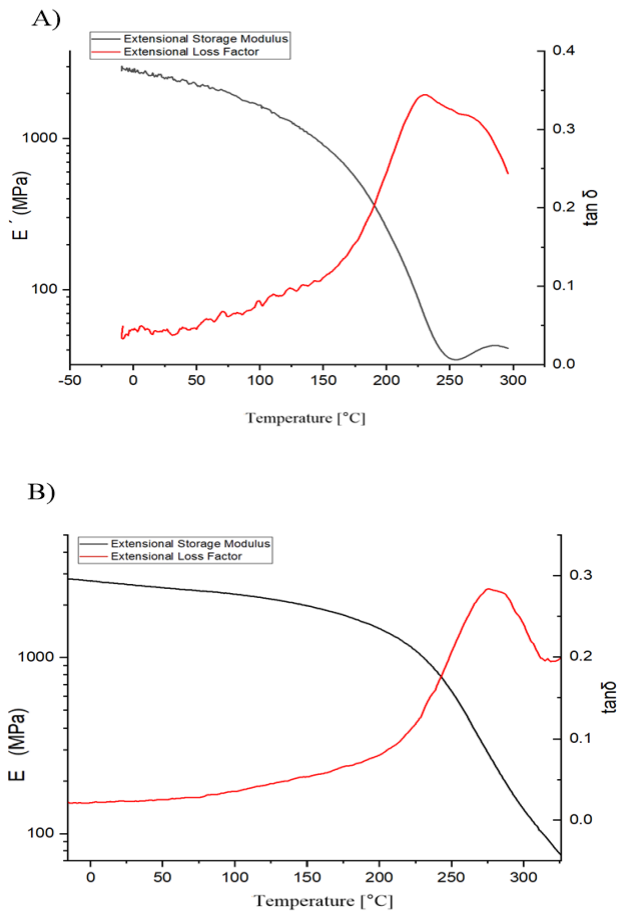

Figure 31 A) second DMA test, B) third DMA test on vitrimer

Glass transition temperature value measured at the peak of tanδ. With each heating cycle, the glass transition temperature (Tg) increased from 247°C to 298°C, suggesting that the crosslinking density of the vitrimer increases at higher temperatures.

This behaviour aligns with the dynamic nature of the vitrimer network, where bond exchange reactions contribute to structural evolution and enhanced crosslinking over time.

3.3.3 Stress relaxation

The stress relaxation test was performed on a sample prepared by curing EV-ODA resin with 3% thermal initiator in a 25 mm diameter circular mould (Figure 32).

Figure 32 Prepared sample for stress relaxation test

Using a dynamic mechanical analyser (DMA) at 150°C (temperature where imine bond exchange becomes active in this material system[42]), a 5% strain was applied and maintained while the stress decay was monitored over time. The resulting data, presented in the Figure 33:

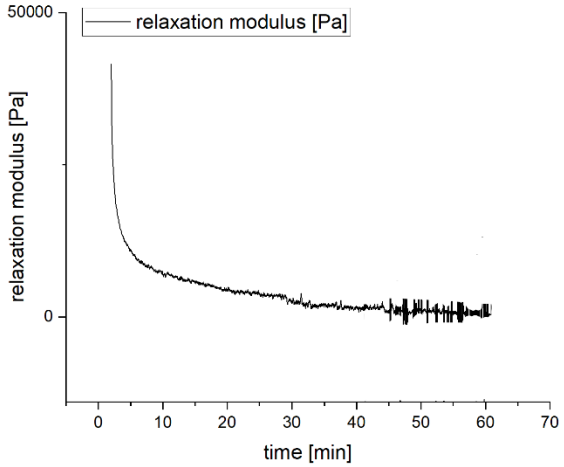

Figure 33 Stress relaxation of vitrimer

The stress relaxation test results demonstrate that the vitrimer begins to undergo noticeable relaxation after approximately one hour at 150°C, indicating the onset of imine bond exchange dynamics.

3.3.4 Tensile test

The tensile strength test samples were prepared by blending EV-ODA resin with 3% thermal initiator in solvent-free conditions, followed by casting into dog bone-shaped moulds. The specimens were then hot-pressed at 150°C for 15 minutes to achieve complete curing.

Figure 34 Hot pressed sample in 150°C for 15 minutes

Figure 34 reveals that the sample remained uncrosslinked after 15 minutes of hot pressing, with visible particulate material present (Figure 34). This is probably due to a not efficient pressure transfer from the press plate to the material. Therefore, a second test was performed using two other pressure plates without a dog-bone shape.

As shown in Figure 35, after curing for another 15 minutes the material convert to very thin (0.2mm), fragile and homogenous film.

Figure 35 Produced film after curing

Rectangular shape with the length of 30mm were cut from this film. Since the film was very fragile and thin, the special clamp was used for tensile test (Figure 36) which has rubbery material instead of usual grip, so the film did not break while clamping it.

Figure 36 Tensile test apparatus

After tensile test, the fractured parts were collected and assembled, then hot pressed at 150 °C for 15 minutes to evaluate the material's reprocessability. The result is shown at Figure 37:

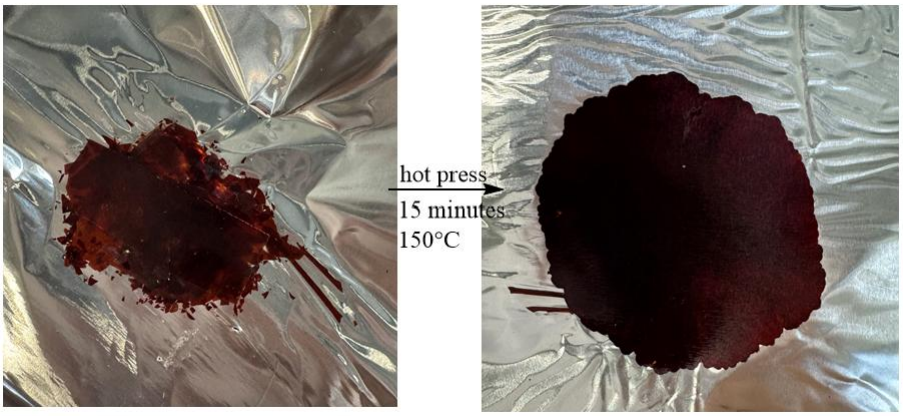

Figure 37 First reprocessing cycle of material

This heating and tensile testing of material performed for four times to show it reprocessability. The resulting stress-strain curves are shown in Figure 38.

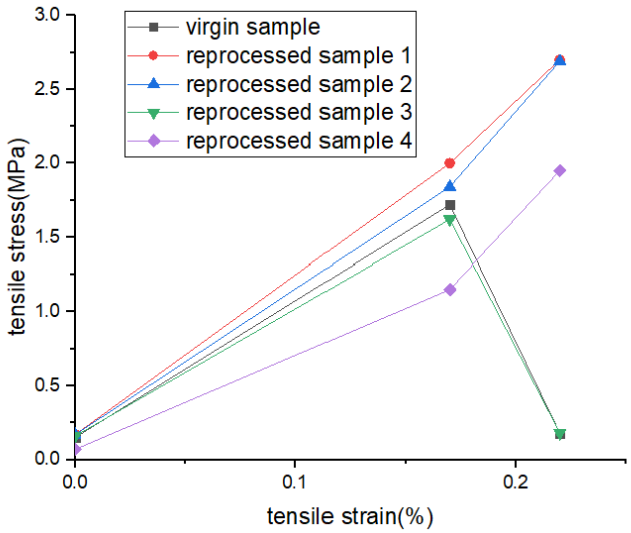

Figure 38 Stress-strain curve

Since the material was fragile, it shows brittle behaviour and failure occurs very soon and does not show the plastic region. The numerous values of stress and strain at break are as following table for each sample:

Table 4 Stress-strain curve data

Sample name	Stress at break [MPa]	Strain at break [%]
Virgin sample	1.72	0.17
Reprocessed sample 1	2.70	0.33
Reprocessed sample 2	2.69	0.33
Reprocessed sample 3	1.62	0.17
Reprocessed sample 4	3.86	0.67

Reprocessed sample 4 has the thickness double than the others,0.4mm, and that is the reason of high stress at break. The young modulus of each sample is written in Table 5:

Table 5 Young modulus of reprocessed material

Sample name	Young modulus [MPa]
Virgin sample	940.04
Reprocessed sample 1	1100.90
Reprocessed sample 2	1002.88
Reprocessed sample 3	874.93
Reprocessed sample 4	646.49

All specimens showed high Young's modulus values, which shows the rigid and cross-linked structure of the polymer. However, a gradual decrease in Young's modulus after each reprocessing cycle was observed. The sample after the fourth cycle of reprocessing showed the lowest modulus, which might be related to the incomplete recovery of crosslinked density.

4 Conclusion

This thesis characterized sustainable and bio-based alternative to fossil-derived polymers with a focus on their material properties.

The intermediate monomer (V-ODA) was synthesized by reaction between vanillin and 4,4' -Oxydianiline. Subsequently, the monomer epoxidized by use of epichlorohydrin (ECH). For synthesize the final polymer the epoxy was mixed with thermal initiator as curing agent and cured for 24 hours in 80 °C.

Synthesized epoxy showed high thermal stability from TGA analysis, showing decomposition temperature around 291°C, compared to the conventional polyimine [43].

In order to thermomechanical evolution of vitrimer the DMA test was performed under repeated thermal cycle. At the first cycle storage modulus decrease by temperature typically, but in 100°C started to increase by increasing temperature unexpectedly which might be due to post-curing. Further tests showed increase in glass transition temperature, which indicated the cross-linking density with each thermal cycle. The material capacity for structural rearrangement and network reinforcement by exchange reaction confirmed by this behaviour.

The stress relaxation behaviour was evaluated by using dynamic mechanical analysis at 150°C, which was chosen according to the literature. In this test a constant strain of 5% was applied at 150°C, and the resulting stress of the material monitored. The vitrimer also exhibited the stress relaxation after 60 minutes which shows that imine bonds undergo to equilibrium exchange reactions. The networks rearranged in certain temperature toward relaxed structure when mechanical stress is applied, which determines the attenuation of the stress response [42].

For performing tensile test, the material was hot pressed twice for 15minutes at 150°C in order to obtain homogenous cross-linked material. After 4 reprocessing cycle at 150°C for 15 minutes each cycle, the material continued to homogenous film and almost same tensile strength. This observation validate the vitrimer potential for sustainable applications.

References

[1] N. R. Council, “Polymer Science and Engineering: The Shifting Research Frontiers,” *Polymer Science and Engineering*, Jan. 1AD, doi: 10.17226/2307.

[2] S. Pourebrahimi and M. Pirooz, “Microplastic pollution in the marine environment: A review,” *Journal of Hazardous Materials Advances*, vol. 10, May 2023, doi: 10.1016/J.HAZADV.2023.100327,AND’,.

[3] A. Shrivastava, “Introduction to Plastics Engineering,” *Introduction to Plastics Engineering*, pp. 1–16, Jan. 2018, doi: 10.1016/B978-0-323-39500-7.00001-0.

[4] “Plastic production in Europe and worldwide 1950-2023| Statista.” Accessed: Apr. 24, 2025. [Online]. Available: https://www.statista.com/statistics/1553461/plastics-production-volume-eu-and-worldwide/

[5] “Thermoplastics and Thermoplastic Composites | ScienceDirect.” Accessed: Apr. 24, 2025. [Online]. Available: https://www-sciencedirect-com.ezproxy.biblio.polito.it/book/9781455778980/thermoplastics-and-thermoplastic-composites

[6] “Materials for Biomedical Engineering | ScienceDirect.” Accessed: Apr. 24, 2025. [Online]. Available: https://www-sciencedirect-com.ezproxy.biblio.polito.it/book/9780128168745/materials-for-biomedical-engineering

[7] N. J. Van Zee and R. Nicolaÿ, “Vitrimers: Permanently crosslinked polymers with dynamic network topology,” *Prog Polym Sci*, vol. 104, p. 101233, May 2020, doi: 10.1016/J.PROGPOLYMSCI.2020.101233.

[8] D. S. Achilias and D. S. Achilias, “Material Recycling - Trends and Perspectives,” *Material Recycling - Trends and Perspectives*, Mar. 2012, doi: 10.5772/2003.

[9] A. J. Peacock and A. Calhoun, “Introduction to Synthetic Polymers,” *Polym Chem*, pp. 1–20, Jan. 2006, doi: 10.3139/9783446433434.001.

[10] I. M. Alarifi, “A comprehensive review on advancements of elastomers for engineering applications,” *Advanced Industrial and Engineering Polymer Research*, vol. 6, no. 4, pp. 451–464, Oct. 2023, doi: 10.1016/J.AIEPR.2023.05.001.

[11] R. Tarodiya and A. Levy, “Surface erosion due to particle-surface interactions - A review,” *Powder Technol*, vol. 387, pp. 527–559, Jul. 2021, doi: 10.1016/J.POWTEC.2021.04.055.

[12] E. Saldívar-Guerra and E. Vivaldo-Lima, “Introduction to Polymers and Polymer Types,” *Handbook of Polymer Synthesis, Characterization, and Processing*, pp. 1–14, Feb. 2013, doi: 10.1002/9781118480793.CH1,AND’,.

[13] J. P. Pascault and R. J. J. Williams, “Overview of thermosets: Present and future,” in *Thermosets: Structure, Properties, and Applications: Second Edition*, Elsevier, 2018, pp. 3–34. doi: 10.1016/B978-0-08-101021-1.00001-0.

[14] P. Shieh *et al.*, “Cleavable comonomers enable degradable, recyclable thermoset plastics,” *Nature*, vol. 583, no. 7817, pp. 542–547, Jul. 2020, doi: 10.1038/s41586-020-2495-2.

[15] S. J. Pickering, “Recycling technologies for thermoset composite materials-current status,” *Compos Part A Appl Sci Manuf*, vol. 37, no. 8, pp. 1206–1215, Aug. 2006, doi: 10.1016/j.compositesa.2005.05.030.

[16] D. J. Fortman, J. P. Brutman, G. X. De Hoe, R. L. Snyder, W. R. Dichtel, and M. A. Hillmyer, “Approaches to Sustainable and Continually Recyclable Cross-Linked Polymers,” *ACS Sustain Chem Eng*, vol. 6, no. 9, pp. 11145–11159, Sep. 2018, doi: 10.1021/ACSSUSCHEMENG.8B02355,AND’,.

[17] V. R. Sastri and G. C. Tesoro, “Reversible crosslinking in epoxy resins. II. New approaches,” *J Appl Polym Sci*, vol. 39, no. 7, pp. 1439–1457, Apr. 1990, doi: 10.1002/APP.1990.070390703;WGROUP:STRING:PUBLICATION.

[18] J. S. Chen, C. K. Ober, M. D. Poliks, Y. Zhang, U. Wiesner, and C. Cohen, “Controlled degradation of epoxy networks: analysis of crosslink density and glass transition temperature changes in thermally reworkable thermosets,” *Polymer (Guildf)*, vol. 45, no. 6, pp. 1939–1950, Mar. 2004, doi: 10.1016/J.POLYMER.2004.01.011.

[19] J. S. Chen, C. K. Ober, and M. D. Poliks, “Characterization of thermally reworkable thermosets: materials for environmentally friendly processing and reuse,” *Polymer (Guildf)*, vol. 43, no. 1, pp. 131–139, Jan. 2002, doi: 10.1016/S0032-3861(01)00605-X.

[20] C. J. Kloxin, T. F. Scott, B. J. Adzima, and C. N. Bowman, “Covalent adaptable networks (CANs): A unique paradigm in cross-linked polymers,” *Macromolecules*, vol. 43, no. 6, pp. 2643–2653, 2010, doi: 10.1021/MA902596S,AND’,.

[21] G. M. Scheutz, J. J. Lessard, M. B. Sims, and B. S. Sumerlin, “Adaptable Crosslinks in Polymeric Materials: Resolving the Intersection of Thermoplastics and Thermosets,” *J Am Chem Soc*, vol. 141, no. 41, pp. 16181–16196, Oct. 2019, doi: 10.1021/jacs.9b07922.

[22] W. Denissen, J. M. Winne, and F. E. Du Prez, “Vitrimers: Permanent organic networks with glass-like fluidity,” *Chem Sci*, vol. 7, no. 1, pp. 30–38, Jan. 2016, doi: 10.1039/c5sc02223a.

[23] M. A. Lucherelli, A. Duval, and L. Avérous, “Biobased vitrimers: Towards sustainable and adaptable performing polymer materials,” *Prog Polym Sci*, vol. 127, Apr. 2022, doi: 10.1016/j.progpolymsci.2022.101515.

[24] B. Krishnakumar, R. V. S. P. Sanka, W. H. Binder, V. Parthasarthy, S. Rana, and N. Karak, “Vitrimers: Associative dynamic covalent adaptive networks in thermoset polymers,” *Chemical Engineering Journal*, vol. 385, p. 123820, Apr. 2020, doi: 10.1016/J.CEJ.2019.123820.

[25] D. Montarnal, M. Capelot, F. Tournilhac, and L. Leibler, “Silica-like malleable materials from permanent organic networks,” *Science (1979)*, vol. 334, no. 6058, pp. 965–968, Nov. 2011, doi: 10.1126/science.1212648.

[26] V. Schenk, K. Labastie, M. Destarac, P. Olivier, and M. Guerre, “Vitrimer composites: current status and future challenges,” *Mater Adv*, vol. 3, no. 22, pp. 8012–8029, Sep. 2022, doi: 10.1039/D2MA00654E,AND’,.

[27] X. Zhang *et al.*, “High-Performance Biobased Vinyl Ester Resin with Schiff Base Derived from Vanillin,” *ACS Appl Polym Mater*, vol. 4, no. 4, pp. 2604–2613, Apr. 2022, doi: 10.1021/ACSAPM.1C01910,AND’,.

[28] A. Roig, P. Hidalgo, X. Ramis, S. De La Flor, and À. Serra, “Vitrimeric Epoxy-Amine Polyimine Networks Based on a Renewable Vanillin Derivative,” *ACS Appl Polym Mater*, vol. 4, no. 12, pp. 9341–9350, Dec. 2022, doi: 10.1021/ACSAPM.2C01604,AND’,.

[29] J. A. Iggo, “NMR spectrometry in inorganic chemistry,” *J Chem Educ*, vol. 78, no. 11, p. 1469, 2001, doi: 10.1021/ED078P1469.2,AND’,.

[30] O. J. . Rees, “Fourier transform infrared spectroscopy : developments, techniques, and applications,” p. 215, 2010.

[31] C. Schick, “Differential scanning calorimetry (DSC) of semicrystalline polymers,” *Anal Bioanal Chem*, vol. 395, no. 6, pp. 1589–1611, Nov. 2009, doi: 10.1007/s00216-009-3169-y.

[32] Matthias. Wagner, “Thermal analysis in practice : fundamental aspects,” 2018.

[33] N. Saadatkhah *et al.*, “Experimental methods in chemical engineering: Thermogravimetric analysis—TGA,” *Canadian Journal of Chemical Engineering*, vol. 98, no. 1, pp. 34–43, Jan. 2020, doi: 10.1002/CJCE.23673,AND’,.

[34] M. P. . Sepe, “Dynamic mechanical analysis for plastics engineering,” p. 189, 1998.

[35] “Polymer Nanocomposites | ScienceDirect.” Accessed: Apr. 30, 2025. [Online]. Available: https://www.sciencedirect.com/book/9781855739697/polymer-nanocomposites

[36] K. P. Menard, *Dynamic-Mechanical Analysis*, 3rd ed. 2020.

[37] S. A. Ashter, “Thermoforming of Single and Multilayer Laminates: Plastic Films Technologies, Testing, and Applications,” *Thermoforming of Single and Multilayer Laminates: Plastic Films Technologies, Testing, and Applications*, pp. 1–326, 2014, doi: 10.1016/C2012-0-02821-9.

[38] “Mechanical and Physical Testing of Biocomposites, Fibre-Reinforced Composites and Hybrid Composites | ScienceDirect.” Accessed: Apr. 30, 2025. [Online]. Available: https://www.sciencedirect.com/book/9780081022924/mechanical-and-physical-testing-of-biocomposites-fibre-reinforced-composites-and-hybrid-composites

[39] “Applied Welding Engineering | ScienceDirect.” Accessed: Apr. 30, 2025. [Online]. Available: https://www.sciencedirect.com/book/9780123919168/applied-welding-engineering

[40] A. B. D. Nandiyanto, R. Oktiani, and R. Ragadhita, “How to read and interpret ftir spectroscope of organic material,” *Indonesian Journal of Science and Technology*, vol. 4, no. 1, pp. 97–118, 2019, doi: 10.17509/IJOST.V4I1.15806.

[41] K. A. Stewart, J. J. Lessard, A. J. Cantor, J. F. Rynk, L. S. Bailey, and B. S. Sumerlin, “High-performance polyimine vitrimers from an aromatic bio-based scaffold,” *RSC Applied Polymers*, vol. 1, no. 1, pp. 10–18, 2023, doi: 10.1039/D3LP00019B,AND’,.

[42] T. Telatin, S. De la Flor, À. Serra, and X. Montané, “Poly(epoxy-imine) vitrimers. Effect of the structure on the stress relaxation and creep resistance,” *Polym Test*, vol. 135, Jun. 2024, doi: 10.1016/j.polymertesting.2024.108465.

[43] T. Türel, K. Saito, I. Glišić, T. Middelhoek, and Ž. Tomović, “RSC Applied Polymers Closing the loop: polyimine thermosets from furfural derived bioresources †,” *Cite this: RSC Appl. Polym*, vol. 2, p. 395, 2024, doi: 10.1039/d3lp00268c.